Combined 147,146 Sm- 143,142 Nd constraints on the longevity and residence time of early terrestrial crust

Antoine Roth, Bernard Bourdon, Stephen Mojzsis, John Rudge, Martin Guitreau, Janne Blichert-Toft

AGU PUBLICATIONS

Geochemistry, Geophysics, Geosystems

RESEARCH ARTICLE
10.1002/2014GC005313

Key Points:
- New ^{147,146}Sm-^{143,142}Nd data are reported for the Acasta Gneiss Complex
- A model age of 4310 Ma is obtained for early enrichment of the Acasta source
- ^{147,146}Sm-^{143,142}Nd constraints on the longevity of early crust are reassessed

Supporting Information:
- ReadMe
- Tables S1–S4

Correspondence to:
A. S. G. Roth,
antoine.roth@space.unibe.ch

Citation:
Roth, A. S. G., B. Bourdon, S. J. Mojzsis, J. F. Rudge, M. Guitreau, and J. Blichert-Toft (2014), Combined ^{147,146}Sm-^{143,142}Nd constraints on the longevity and residence time of early terrestrial crust, *Geochem. Geophys. Geosyst.*, *15*, 2329–2345, doi:10.1002/2014GC005313.

Received 21 FEB 2014
Accepted 5 MAY 2014
Accepted article online 7 MAY 2014
Published online 10 JUN 2014

Combined ^{147,146}Sm-^{143,142}Nd constraints on the longevity and residence time of early terrestrial crust

Antoine S. G. Roth[1,2], Bernard Bourdon[3], Stephen J. Mojzsis[3,4,5,6], John F. Rudge[7], Martin Guitreau[3,8], and Janne Blichert-Toft[3]

[1]Institute of Geochemistry and Petrology, ETH Zurich, Zurich, Switzerland, [2]Now at Institute of Physics, University of Bern, Bern, Switzerland, [3]Laboratoire de Géologie de Lyon, ENS Lyon and UCBL, UMR 5276, CNRS, Lyon, France, [4]Department of Geological Sciences, University of Colorado, Boulder, Colorado, USA, [5]NASA Lunar Science Institute, Center for Lunar Origin and Evolution, USA, [6]Institute for Geological and Geochemical Research, Research Center for Astronomy and Earth Sciences, Hungarian Academy of Sciences, Budapest, Hungary, [7]Bullard Laboratories, Department of Earth Sciences, University of Cambridge, Cambridge, UK, [8]CEPS-Department of Earth Sciences, University of New Hampshire, Durham, New Hampshire, USA

Abstract Primordial silicate differentiation controlled the composition of Earth's oldest crust. Inherited ^{142}Nd anomalies in Archean rocks are vestiges of the mantle-crust differentiation before ca. 4300 Ma. Here we report new whole-rock ^{147,146}Sm-^{143,142}Nd data for the Acasta Gneiss Complex (AGC; Northwest Territories, Canada). Our ^{147}Sm-^{143}Nd data combined with literature data define an age of 3371 ± 141 Ma (2 SD) and yield an initial ε^{143}Nd of −5.6 ± 2.1. These results are at odds with the Acasta zircon U-Pb record, which comprises emplacement ages of 3920–3960 Ma. Ten of our thirteen samples show ^{142}Nd deficits of −9.6 ± 4.8 ppm (2 SD) relative to the modern Earth. The discrepancy between ^{142}Nd anomalies and a mid-Archean ^{147}Sm-^{143}Nd age can be reconciled with Nd isotope reequilibration of the AGC during metamorphic perturbations at ca. 3400 Ma. A model age of ca. 4310 Ma is derived for the early enrichment of the Acasta source. Two compositional end-members can be identified: a felsic component with ^{142}Nd/^{144}Nd identical to the modern Earth and a mafic component with ^{142}Nd/^{144}Nd as low as −14.1 ppm. The ca. 4310 Ma AGC source is ~200 Myr younger than those estimated for Nuvvuagittuq (northern Québec) and Isua (Itsaq Gneiss Complex, West Greenland). The AGC does not have the same decoupled Nd-Hf isotope systematics as these other two terranes, which have been attributed to the crystallization of an early magma ocean. The Acasta signature rather is ascribed to the formation of Hadean crust that was preserved for several hundred Myr. Its longevity can be linked to ^{142}Nd evolution in the mantle and does not require slow mantle stirring times nor modification of its convective mode.

1. Introduction

The last vestiges of planetary-scale Hadean silicate differentiation are preserved in some Archean rocks, notably in the form of anomalies in the relative abundance of radiogenic ^{142}Nd, the decay product of short-lived nuclide ^{146}Sm (half-life $T_{1/2}$ = 68 Myr) [*Kinoshita et al.*, 2012]. Small but detectable variations in ^{142}Nd against ^{144}Nd result from fractionation of Sm and Nd during magmatic processes that took place prior to about 4300 Ma. The magnitude of this fractionation was limited because Sm and Nd are both light rare earth elements (REE) and thus have similar chemical properties. The initial Solar System abundance of ^{146}Sm was low (^{146}Sm/^{144}Sm = 9.5 × 10^{-3}) [*Kinoshita et al.*, 2012], hence restricting the ingrowth of ^{142}Nd. Yet the ^{146}Sm-^{142}Nd chronometer has proven to be a sensitive tracer of early silicate Earth differentiation and it is often assumed that this system, unlike the ^{147}Sm-^{143}Nd system, is less affected by later events. Modeling of the combined ^{146}Sm-^{142}Nd and ^{147}Sm-^{143}Nd systematics in the Eoarchean (ca. 3780 Ma) [*Cates et al.*, 2013] Nuvvuagittuq supracrustal belt in northern Québec has shown that later perturbations could have disturbed early radiogenic signatures preserved in the oldest rocks, thereby complicating their interpretation [*Roth et al.*, 2013; cf. *O'Neil et al.*, 2012]. One approach to overcome this problem is to combine the Sm-Nd isotope systems with other radiogenic chronometers, such as the long-lived ^{176}Lu-^{176}Hf system and U-Pb zircon geochronology [e.g., *Guitreau et al.*, 2013]. The well-documented antiquity of the Acasta Gneiss Complex (AGC; Northwest Territories, Canada) renders it the key locality where such an integrated approach could provide insights into processes taking place in the formative stages of Earth history. Some of the unresolved issues about Acasta are the discrepancy between old U-Pb zircon ages and the younger ^{147}Sm-^{143}Nd

record and the implications of the highly enriched (unradiogenic) $^{143}Nd/^{144}Nd$ compositions observed in AGC rocks [e.g., *Mojzsis et al*., 2014].

Captured in the westernmost Slave Craton (Canada), the AGC is a remnant late-Hadean/Eoarchean terrane consisting of a complex assemblage of strongly deformed rocks with different igneous protolith ages [*Bowring et al*., 1989a; *Bowring and Housh*, 1995; *Bleeker and Stern*, 1997; *Stern and Bleeker*, 1998; *Bowring and Williams*, 1999; *Sano et al*., 1999]. The Acasta gneisses preserve U-Pb zircon emplacement ages that broadly fall into three groups: ca. 3960–3920 Ma, ca. 3850–3720 Ma, and 3660–3590 Ma [*Iizuka et al*., 2007; *Mojzsis et al*., 2014]. The oldest of these have ages that span ca. 4020–4050 Ma [*Bowring and Williams*, 1999; *Stern and Bleeker*, 1998], and in rare cases up to about 4200 Ma [*Iizuka et al*., 2006]; these ages are for zircon xenocrysts in the AGC granitoids resulting from incomplete assimilation of older, mafic, precursors [*Mojzsis et al*., 2014].

Based on their ^{147}Sm-^{143}Nd study of two gneissic samples, *Bowring et al*. [1989b] reported a chondritic uniform reservoir (CHUR) model age of 4100 Ma and an initial $\varepsilon^{143}Nd$ at 3700 Ma of -4.8 for the AGC. At the time this was the oldest chondritic model age yet reported for a terrestrial sample, and it was interpreted as evidence for the preservation of an early-enriched crust. Subsequent comprehensive whole-rock ^{147}Sm-^{143}Nd work on Acasta rocks, however, yielded a much younger regression age of ca. 3300 Ma [*Bowring and Housh*, 1995; *Moorbath et al*., 1997; *Mojzsis et al*., 2014]. These "errorchrons" have been interpreted as either the age of resetting of the ^{147}Sm-^{143}Nd chronometer corresponding to large scale Nd isotope homogenization of Acasta gneisses at ca. 3300 Ma [*Moorbath et al*., 1997; *Whitehouse et al*., 2001], or a mixing line with no age significance [*Bowring and Housh*, 1995]. *Bowring et al*. [1990] and *Bowring and Housh* [1995] attributed the large range in initial $\varepsilon^{143}Nd$ from -4.8 to $+3.6$ (calculated using the ages obtained from zircon U-Pb geochronology) to major Hadean mantle heterogeneities. Alternatively, *Moorbath et al*. [1997] and *Whitehouse et al*. [2001] argued that resetting of the Sm-Nd system makes the calculation of initial $\varepsilon^{143}Nd$ based on zircon U-Pb ages geologically irrelevant. They instead interpreted the negative initial $\varepsilon^{143}Nd$ value of -5.7 ± 0.7, calculated with the age given by the ^{147}Sm-^{143}Nd errorchron, as independent support for early enrichment of the Acasta protoliths [see also *Guitreau et al*., 2014].

The first ^{146}Sm-^{142}Nd studies of Acasta showed no ^{142}Nd evidence for early differentiation. *McCulloch and Bennett* [1993] and *Caro et al*. [2006] conducted ^{142}Nd measurements on three Acasta samples (92–179, SP-405, and SM/Ac/18) and reported $^{142}Nd/^{144}Nd$ values within error of the modern terrestrial composition. Samples 92–179 and SP-405 were two granitoid gneisses both with a zircon U-Pb age of 3962 ± 3 Ma [*Bowring et al*., 1989b; *Williams et al*., 1992] and $\varepsilon^{143}Nd$ at 3962 Ma of $+2.5$ and $+0.8$, respectively [*Bennett et al*., 1993; *Bowring et al*., 1990]. Sample SM/Ac/18 was a hornblende-plagioclase schist ("leucogabbro" *s.l.* of *Mojzsis et al*. [2014]) of uncertain provenance with $^{147}Sm/^{144}Nd$ and $^{143}Nd/^{144}Nd$ of 0.1212 and 0.510721, respectively [*Moorbath et al*., 1997].

Iizuka et al. [2009] subsequently reported in situ Lu-Hf isotope analyses of zircons for five Acasta granitoid gneisses with U-Pb zircon ages between ca. 3590 and 3970 Ma. Magmatic zircons yielded negative initial $\varepsilon^{176}Hf$ ranging from -6.1 to -1.2. This result was consistent with the presence of zircon xenocrysts as old as 4200 Ma in certain samples [*Iizuka et al*., 2006, 2007] and suggested that some AGC gneisses had interacted with Hadean crust. This conclusion is supported by the now-established inheritance of pre-3960 Ma Acasta zircons [*Mojzsis et al*., 2014], and by whole-rock Lu-Hf isotope data [*Guitreau et al*., 2014].

To better understand the formation history of the AGC and thereby the significance of its discordant ^{147}Sm-^{143}Nd systematics and its zircon U-Pb geochronology, high-precision whole-rock $^{147,146}Sm$-$^{143,142}Nd$ data were obtained on samples that had already been studied in detail for Lu-Hf isotope systematics in zircons and whole-rocks by *Guitreau et al.* [2012, 2014], and for U-Pb in zircons by *Mojzsis et al*. [2014]. The new $^{147,146}Sm$-$^{143,142}Nd$ data were compared to literature ^{147}Sm-^{143}Nd [*Bowring and Housh*, 1995; *Moorbath et al*., 1997] and ^{146}Sm-^{142}Nd [*McCulloch and Bennett*, 1993; *Caro et al*., 2006] data for Acasta and to the new Lu-Hf isotope data by *Guitreau et al*. [2014]. The principal goals with this work were to (1) assess whether Acasta rocks have preserved ^{142}Nd evidence for early mantle-crust differentiation, (2) characterize the Acasta source using the $^{147,146}Sm$-$^{143,142}Nd$ systematics as tracers in light of the new Lu-Hf isotope data, and (3) reassess the longevity of early terrestrial crust during the Hadean and Archean, and its implications for the evolution of the mantle-crust system.

2. Geological Setting and Sample Description

The Acasta Gneiss Complex was discovered in the early 1980s during regional mapping by the Geological Survey of Canada [*King*, 1985; *St-Onge et al*., 1988; and references therein]. It is located at the western margin of the Slave Craton approximately 300 km north of Yellowknife (town) in the Northwest Territories of Canada. The actual extent of the Acasta outcrops remains unknown and thus far only a small area within one of several domal basement antiforms composing the terrane have been investigated in finer detail [e.g., *Iizuka et al*., 2006].

Our sample set comprises eleven granitoid gneisses and two hornblende-plagioclase schists collected in the course of high-resolution (1:50 scale) mapping of individual outcrops within the Acasta complex. We selected these rocks because of their old (Hadean-Eoarchean) U-Pb zircon ages or their negative initial ε^{176}Hf, each of which would suggest that they may have preserved ^{142}Nd evidence of early silicate differentiation. Granitoid gneisses are quartz-bearing, hornblende-bearing, and biotite-bearing rocks and can be separated into (i) a "silica-poor" tonalitic group with $SiO_2 \leq 60$ wt % (AG09008 and AG09017), (ii) an "intermediate" tonalitic group with 65–70 wt % SiO_2 (AG09014 and AG09016), and (iii) a "granitic" group with $SiO_2 \geq 70$ wt % (AG09009). They have typical tonalite-trondhjemite-granodiorite compositions with light rare earth element (LREE) enrichments and heavy rare earth element (HREE) depletions (normalized to chondrite), small negative Eu anomalies, and negative Nb and Ti anomalies relative to primitive mantle. Hornblende-plagioclase schists are silica-poor ($\sim$44 wt % SiO_2) and have comparatively flat LREE/HREE patterns, positive Eu anomalies, small positive Nb and large positive Ti anomalies relative to primitive mantle, indicating that the protolith of these rocks was a cumulate. More detailed lithological descriptions of the samples are provided in *Mojzsis et al*. [2014] and *Guitreau et al*. [2014].

The U-Pb zircon ages of these samples fall into the age groups previously defined by *Iizuka et al*. [2007]. The oldest granitoid gneiss samples AG09005, −06, −17, −30, −31, −16, and −08g have ages of ca. 3920–3960 Ma; other gneisses, AG09001 and −08, have an intermediate age of ca. 3750 Ma; and the youngest (AG09014, −22) are ca. 3600 Ma. Although of uncertain age, the plagioclase-hornblende schists AG09017N and −20 are present as enclaves within the oldest ca. 3960 Ma granitoid gneisses, and are therefore the oldest recognized components of the AGC [*Stern and Bleeker*, 1998]. *Guitreau et al*. [2014] showed that based on Lu-Hf isotope systematics sample AG09020 (a hornblende-plagioclase schist) is likely to be about 3960 Ma.

3. Methods

3.1. Sample Preparation

The measurement of Nd isotope ratios and Sm and Nd concentrations in bulk rock samples required the chemical separation and purification of the two REEs. The method for the preparation of 100–250 mg of powdered rocks containing about 1 μg of Nd is given in *Roth et al*. [2013], which in turn was adapted from *Caro et al*. [2006]. Each sample was digested in a concentrated HF-HNO_3 mixture. The fluorides were completely eliminated after fuming with a few μl of $HClO_4$. The residue was then taken up several times in HCl until obtaining a clear solution. An aliquot of 2–5% was pipetted out and spiked with an optimized amount of ^{150}Nd-^{149}Sm tracer for the determination of Sm and Nd concentrations by isotope dilution. Samarium and Nd were extracted from the bulk rock solution as follows: (1) The REE fraction was separated from the rock matrix by ion chromatography on a TRU-Spec resin. (2) Cerium—which interferes on mass 142 during the measurement of Nd isotopes—was efficiently removed and discarded from the other REEs by a solvent extraction technique [*Rehkämper et al*., 1996]. (3) The Ce-free REE fraction was further purified on an AG50W-X8 cation-exchange resin and cleaned of Na, an additive element introduced as sodium bromate during step 2 [cf. *Rehkämper et al*., 1996]. (4) Purified Sm and Nd were finally separated on Ln-Spec resin and collected individually. The preparation of the spiked aliquots followed the same procedure but omitting steps 2 and 3 as small isobaric interferences of Ce on Sm and Nd isotope masses are negligible during isotope dilution mass spectrometry.

3.2. Measurements of Nd Isotope Ratios and Sm and Nd Concentrations

The measurements of Nd isotope ratios were performed by thermal ionization (Nd^+) using a Thermo Triton (TIMS) at ETH Zurich [*Roth et al*., 2013]. About 500 ng of Nd and 200 ng of H_3PO_4 (activator) were loaded onto the evaporation filament of a double rhenium assembly. A ^{142}Nd ion beam of about 7.5 V (using 10^{11} Ω

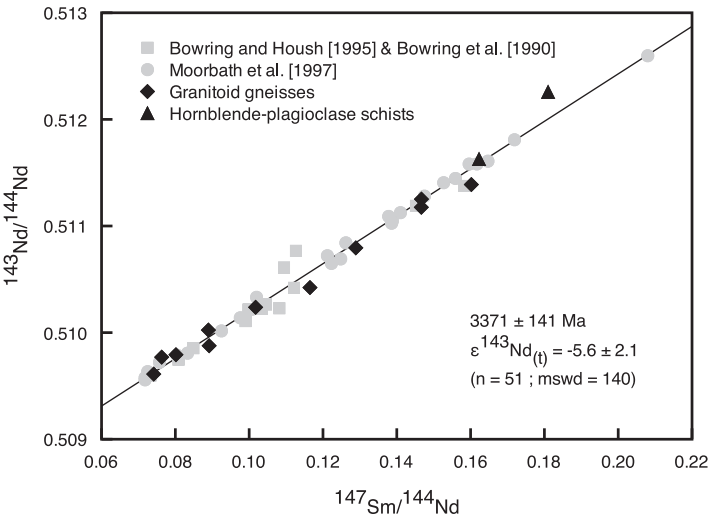

Figure 1. ^{147}Sm-^{143}Nd (long lived) isochron diagram for the Acasta samples. The Acasta samples from this study (black symbols) were combined with those of *Bowring* and *Housh* [1995], *Bowring et al.* [1990], and *Moorbath et al.* [1997] (gray symbols). Analytical uncertainties are about the size of the symbols. The solid line represents the best fit to the combined data sets.

feedback resistors) was obtained when the ionization filament was heated with a current of 5500 mA and the evaporation filament typically adjusted to 1600 mA. A multidynamic acquisition scheme using two magnet settings lowered to negligible levels the effect of variability in efficiency among the detectors on the measured isotope ratios. The contributions of Ce and Sm isobaric interferences on, respectively, ^{142}Nd and ^{144}Nd never exceeded 2 ppm. They were monitored with, respectively, ^{140}Ce and ^{147}Sm and corrected for online. Neodymium isotope ratios were corrected for mass fractionation using the exponential law and a ^{146}Nd/^{144}Nd reference value of 0.7219. The thirteen repeated measurements of the JNdi-1 standard gave a mean ^{142}Nd/^{144}Nd value of 1.1418370 $\pm$ 0.0000049 (2 SD) with an external precision of $\pm$4.3 ppm, which is identical within errors to the value of 1.1418351 $\pm$ 0.0000042 reported by *Roth et al.* [2013]. Table S1 lists the Nd isotope ratios for the Acasta samples and the JNdi-1 standards.

Samarium and Nd concentrations were determined by isotope dilution mass spectrometry. The measurements of the isotopic compositions of the spiked aliquots were done using a Nu Instruments MC-ICP-MS at ETH Zurich [*Roth et al*., 2013]. Table S1 lists the concentrations of Sm and Nd for the Acasta samples.

4. Results

The new Acasta ^{147,146}Sm-^{143,142}Nd whole-rock data obtained for the eleven granitoid gneisses and two plagioclase-hornblende schists are reported in Table S1.

In a ^{147}Sm-^{143}Nd isochron diagram (Figure 1), the Acasta samples analyzed in this study fall on the same array as that previously reported by *Bowring and Housh* [1995], *Moorbath et al*. [1997], and *Mojzsis et al*. [2014]. The ^{147}Sm/^{144}Nd ratios of the present samples, similar to the samples reported in the literature, also show a broad range from very low (0.0741) to subchondritic (0.1810) values. Likewise, ^{143}Nd/^{144}Nd ratios range from 0.509611 for the least radiogenic granitoid gneiss to 0.512256 for the most radiogenic plagioclase-hornblende schist. The combined data sets define an errorchron (MSWD = 140) with an age of 3371 $\pm$ 141 Ma and yield an initial ^{143}Nd/^{144}Nd value of 0.507976 $\pm$ 0.000106. This translates into ε^{143}Nd of -5.6 ± 2.1 when normalized to CHUR [*Bouvier et al*., 2008] and -7.3 ± 2.1 when using a superchondritic terrestrial composition as defined by *Caro and Bourdon* [2010].

Unlike previous reports [*McCulloch and Bennett*, 1993; *Caro et al*., 2006], ten out of the thirteen Acasta samples measured here have ^{142}Nd anomalies (Figure 2). This difference in our results can be rationalized by the fact that the samples analyzed in the present study were specifically chosen based on their field relationships (single lithotype), U-Pb zircon geochronology (uncomplicated zircon populations), and their undisturbed Lu-Hf isotope systematics to have had a relatively well-preserved ancient history. Figure 2 shows the ^{142}Nd/^{144}Nd ratios expressed as ppm deviations from the JNdi-1 standard (assumed to be equal to the

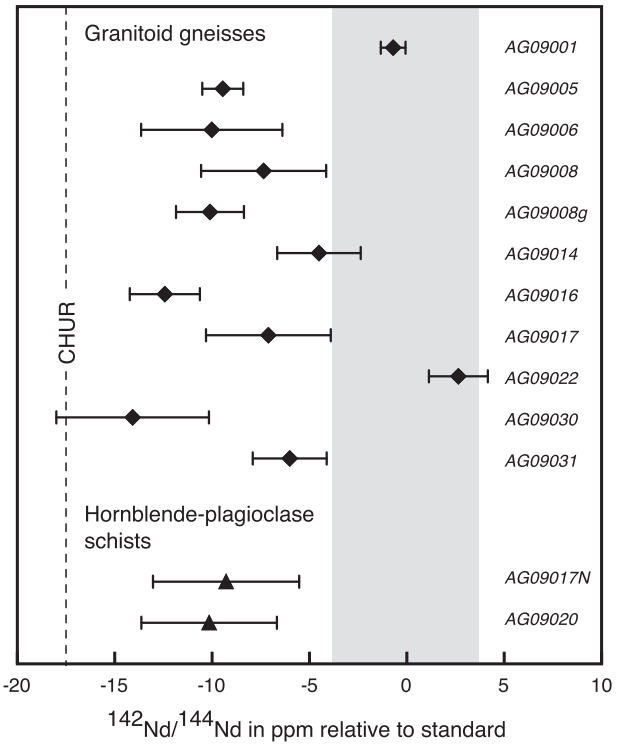

Figure 2. Deviation expressed in parts per million (ppm) of the $^{142}Nd/^{144}Nd$ for the Acasta samples relative to the JNdi-1 Nd standard. The gray band shows the external precision of 4.3 ppm (2 SD) and the dashed line the composition of the chondritic uniform reservoir (CHUR) [*Bouvier et al.*, 2008]. Sample names are labeled in italics. Analytical uncertainties are defined as the 2 SD of the repeated measurements or the 2 SE of the internal run for samples analyzed only once. The granitoid gneisses AG09001, −14, and −22 have identical $^{142}Nd/^{144}Nd$ within errors to the terrestrial standard. All other analyzed Acasta samples show resolvable ^{142}Nd deficits between −6.0 and −14.1 ppm.

modern terrestrial value). The three younger granitoid gneisses AG09001, −14, and −22 have $^{142}Nd/^{144}Nd$ identical within errors to the terrestrial standard. All other analyzed Acasta samples show resolvable ^{142}Nd deficits ranging from −6.0 to −14.1 ppm. When pooled they have a mean $^{142}Nd/^{144}Nd$ value of −9.6 ± 4.8 ppm (2 SD).

The $^{142}Nd/^{144}Nd$ data plotted against $^{147}Sm/^{144}Nd$ (Figure 3) for the Acasta samples analyzed here do not define an errorchron similar to that observed in the ^{147}Sm-^{143}Nd isochron diagram (Figure 1). The three granitoid gneisses AG09001, −14, and −22 with $^{142}Nd/^{144}Nd$ identical to the standard have very low $^{147}Sm/^{144}Nd$ varying from 0.0741 to 0.0802. Acasta samples with ^{142}Nd deficits have higher $^{147}Sm/^{144}Nd$ that span an interval from 0.0890 to 0.1810, corresponding to more mafic lithologies. We find that $^{142}Nd/^{144}Nd$ does not correlate with $^{147}Sm/^{144}Nd$. When pooled these data yield a mean $^{142}Nd/^{144}Nd$ value of 1.141826 ± 0.000006 (2 SD).

The $^{142}Nd/^{144}Nd$ data plotted against major and trace element concentrations (Figure 4) show systematic trends. We find that $^{142}Nd/^{144}Nd$ correlates positively with Nd, SiO_2, and Na_2O concentrations and negatively with Fe_2O_3, MgO, and

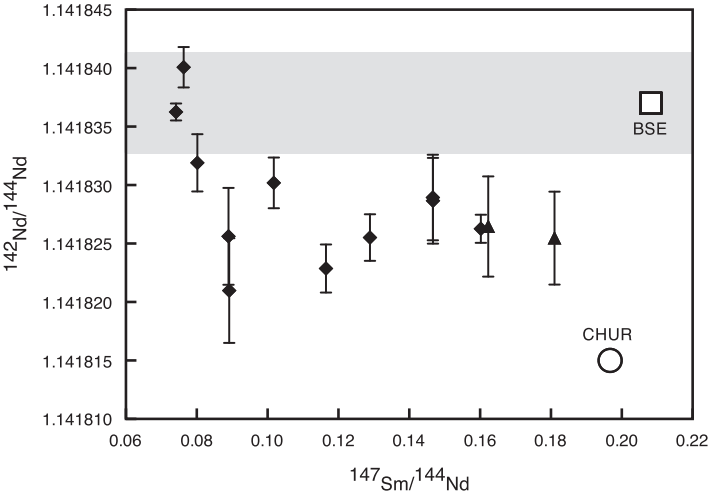

Figure 3. ^{146}Sm-^{142}Nd (short lived) isochron diagram for Acasta samples. The gray band shows the external precision of 4.3 ppm (2 SD); the square symbol the composition of the superchondritic bulk silicate Earth (BSE) [*Caro and Bourdon*, 2010]; and the round symbol the composition of the chondritic uniform reservoir (CHUR) [*Bouvier et al.*, 2008]. Analytical uncertainties are defined as the 2 SD of the repeated measurements or the 2 SE of the internal run for samples analyzed only once.

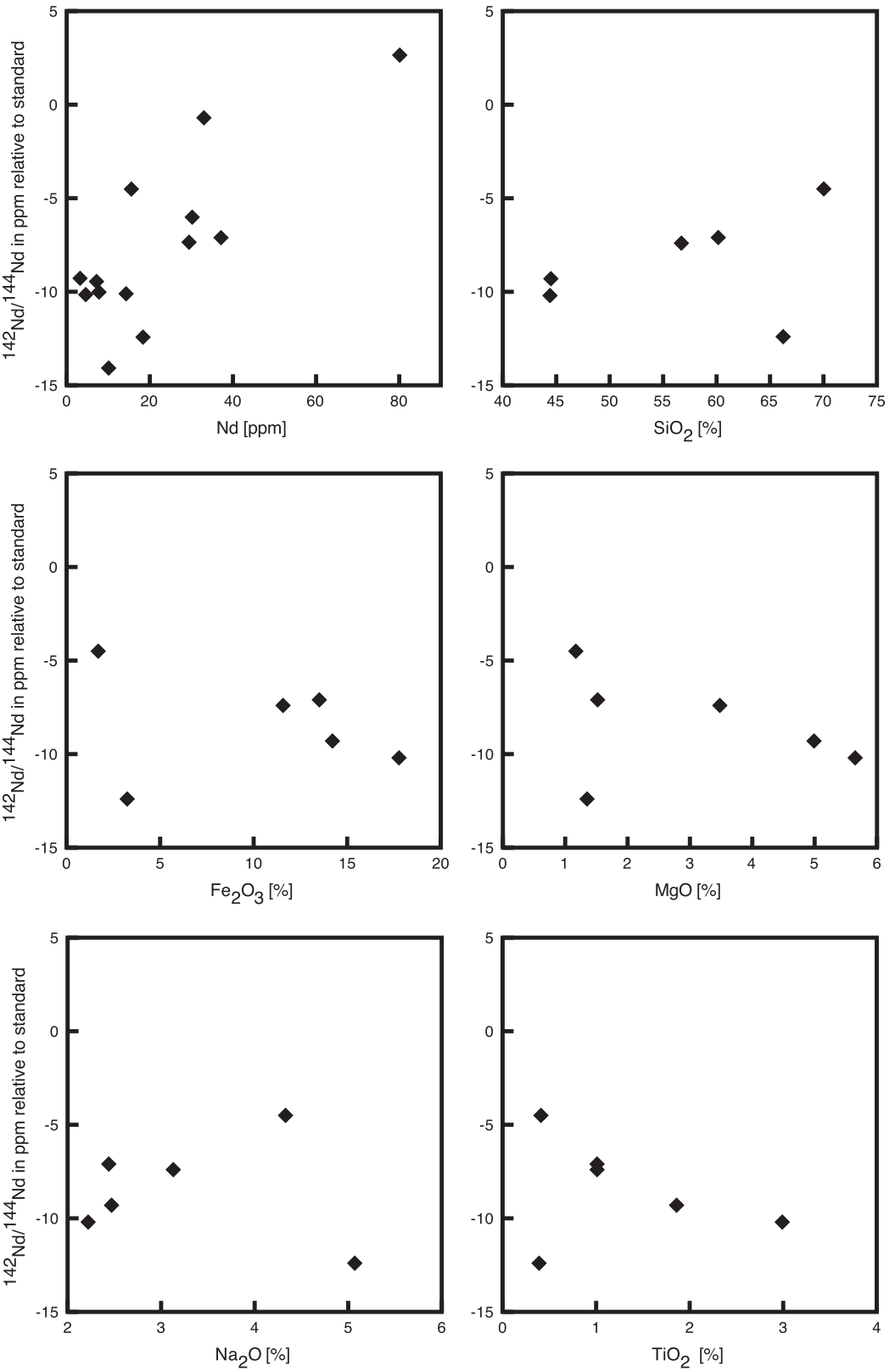

Figure 4. $^{142}Nd/^{144}Nd$ versus Nd and major element concentrations. Only samples AG09008, −14, −16, −17, −17N, and −20 are plotted for the major elements because chemical composition data for the other Acasta samples are not available. Sample AG09016, a granitoid gneiss, is a systematic outlier in all the trends.

TiO_2 concentrations. These observations strongly suggest that the ultimate source of the oldest Acasta component is mafic rather than felsic, which is consistent with the conclusions of *Mojzsis et al*. [2014] and *Guitreau et al*. [2014]. The ca. 3920–3960 Ma granitoid gneiss AG09016 with a low $^{142}Nd/^{144}Nd$ of −12.4 ppm falls systematically off all trends. We note that this rock corresponds to the sample for which *Iizuka et al*. [2007] reported ca. 4200 Ma U-Pb ages in zircon cores. It is also noteworthy that this sample contains primary muscovite [*Guitreau et al*., 2012], and is plausibly derived from anatexis of evolved crust.

5. Discussion

5.1. ^{147}Sm-^{143}Nd Systematics

As shown by *Moorbath et al*. [1997], it cannot be fortuitous for Acasta rocks with differences in U-Pb zircon ages of up to ∼400 Myr and differences in initial $\varepsilon^{143}Nd$ of up to 8 ε units [*Bowring and Housh*, 1995] to delineate a correlation in a ^{147}Sm-^{143}Nd isochron diagram. Thus, we interpret the 3371 ± 141 Ma "age" defined by the ^{147}Sm-^{143}Nd errorchron (Figure 1) as the time of the last metamorphic event that homogenized Nd isotopes in the Acasta rocks [*Moorbath et al*., 1997; *Whitehouse et al*., 2001]. This age is similar to those of a few zircon overgrowths that date high-grade metamorphism and Pb-loss from magmatic zircons [*Bleeker and Stern*, 1997]. It also roughly agrees within uncertainties with the Lu-Hf age of 3681 ± 352 Ma reported by *Guitreau et al*. [2014] for the same samples. Negative initial $\varepsilon^{143}Nd$ and $\varepsilon^{176}Hf$ of, respectively, −5.6 ± 2.1 (Figure 1) and −4.8 ± 3.4 [*Guitreau et al*., 2014] indicate that ^{147}Sm-^{143}Nd and ^{176}Lu-^{176}Hf are consistent with each other and record an early enrichment of the Acasta protoliths, although the ^{147}Sm-^{143}Nd system shows evidence of resetting.

5.2. ^{146}Sm-^{142}Nd Systematics

Ten Acasta samples have ^{142}Nd deficits that range from −6.0 to −14.1 ppm and only three samples (AG09001, −14, and −22) have $^{142}Nd/^{144}Nd$ identical to the terrestrial standard representing the bulk silicate Earth composition (Figure 2). Notably, these three samples have the lowest $^{147}Sm/^{144}Nd$ ratios and thus correspond to the most felsic rocks analyzed (Figure 3). This more felsic character is also illustrated by the correlation of $^{142}Nd/^{144}Nd$ with major element concentrations (Figure 4). Samples AG09014 and −22 have young zircon U-Pb ages of ca. 3600 Ma, while sample AG09001 has an intermediate age of ca. 3750 Ma. All Acasta samples with ^{142}Nd deficits have old ages of ca. 3960 Ma; sample AG09008 is problematic with an estimated age of ca. 3750 Ma [*Mojzsis et al*., 2014; *Guitreau et al*., 2012]. Samples AG09001, −14, and −22 could be derived from a younger geological unit that inherited $^{142}Nd/^{144}Nd$ ratios identical to the bulk silicate Earth.

The ^{146}Sm-^{142}Nd systematics show that the oldest Acasta rocks with an age of ca. 3960 Ma have a mean ^{142}Nd deficit of −9.6 ± 4.8 ppm (2 SD). Owing to the fact that radioactive ^{146}Sm was already extinct when these rocks formed, they must have inherited their unradiogenic $^{142}Nd/^{144}Nd$ from a much older enriched Hadean source. Early enrichment of Acasta has already been attested to by ^{147}Sm-^{143}Nd [*Bowring et al*., 1989b; *Moorbath et al*., 1997; *Whitehouse et al*., 2001; *Mojzsis et al*., 2014] and ^{176}Lu-^{176}Hf [*Guitreau et al*., 2014] in whole-rocks, ^{176}Lu-^{176}Hf in zircons [*Iizuka et al*., 2009], and the occurrence of up to ca. 4200 Ma zircon xenocrysts in the oldest rocks [*Iizuka et al*., 2006]. We note that it is difficult to define precisely the age of the enrichment event corresponding to the Sm/Nd fractionation leading to the observed Nd isotopic signature simply based on the ^{147}Sm-^{143}Nd system. This can more readily be achieved by combining the ^{147}Sm-^{143}Nd and ^{146}Sm-^{142}Nd systems.

5.3. Coupled $^{147,146}Sm$-$^{143,142}Nd$ Systematics

The ^{147}Sm-^{143}Nd systematics for Acasta rocks suggest that a metamorphic event reset, at least partially, $^{143}Nd/^{144}Nd$ at 3371 Ma. It is likely that $^{142}Nd/^{144}Nd$ was also affected by this event. The younger Acasta samples have the most felsic composition and no ^{142}Nd deficits. In contrast, older Acasta samples all have more mafic compositions and show ^{142}Nd deficits in a relatively restricted range of −9.6 ± 4.8 ppm (2 SD). This indicates that partial resetting of ^{143}Nd likely also modified the ^{142}Nd systematics.

Based on the calculated initial $^{143}Nd/^{144}Nd$ and $^{142}Nd/^{144}Nd$ ratios at 3371 Ma, it is possible to determine independently a model age of Sm-Nd fractionation starting from a BSE composition using a simple two-stage model for the Nd isotope evolution. For this purpose, we assumed that the precursor material of Acasta evolved until the age of fractionation (T_f) with a BSE composition. At T_f, the formation of crust yields

a new Sm/Nd ratio lower than that of the BSE [e.g., *Caro and Bourdon*, 2010]. Coupling the ^{147,146}Sm-^{143,142}Nd systematics and using an initial ^{143}Nd/^{144}Nd of 0.507976 and an initial ^{142}Nd/^{144}Nd of 1.141824 for the rocks with ^{142}Nd deficits yields a model age of 4350 Ma and a ^{147}Sm/^{144}Nd ratio of 0.1505 for the Acasta source. If there were any variability in the abundance of ^{142}Nd/^{144}Nd due to variations in Sm/Nd in the protoliths of these rocks, the later event seems for the most part to have erased it. The effect of this event is to homogenize the ^{142}Nd/^{144}Nd ratios of the rocks to a value close to the bulk composition. A similar calculation can be made for the Lu-Hf isotope system assuming that a common event fractionated the ^{176}Lu/^{177}Hf ratio at 4350 Ma. Using an initial ^{176}Hf/^{177}Hf of 0.2802 (at 3945 Ma) for Acasta [*Guitreau et al.*, 2014], the corresponding ^{176}Lu/^{177}Hf of the AGC source would be 0.029. One should note that the ^{147}Sm/^{144}Nd and ^{176}Lu/^{177}Hf ratios obtained for the Acasta source fall within the range of those measured in the rocks. In summary, our modeling shows that the Sm-Nd systematics of the Acasta rocks can be explained by an early Sm/Nd fractionation at 4350 Ma followed by a later thermal event that (partially) reset the Nd isotopic signatures at ~3400 Ma. We find that similar to the Nuvvuagittuq supracrustal belt [*Roth et al.*, 2013], negative ^{142}Nd anomalies were inherited from the Hadean and preserved within the crust for several hundred million years.

5.4. A Scenario for the Formation of the Acasta Gneiss Complex

Trends of ^{142}Nd/^{144}Nd as a function of Nd and major element concentrations (Figure 4) reveal that the Acasta source consists of two end-members. One is felsic in composition and has a ^{142}Nd/^{144}Nd value identical to the modern BSE value. The other is mafic and characterized by lower SiO_2 and Al_2O_3 and higher MgO and has ^{142}Nd/^{144}Nd with a mean value of -9.6 ± 4.8 ppm. Sample AG09016 with low ^{142}Nd/^{144}Nd of ~12.4 ppm falls off all trends and possibly represents an Eoarchean partial melt of a Hadean end-member. Alternatively, it could represent a high degree of crustal contamination, which is supported by the observations of ca. 4000–4200 Ma zircon xenocrysts. In the following section, we focus on the origin of this ancient mafic end-member.

The ^{143}Nd/^{144}Nd and ^{142}Nd/^{144}Nd isotope evolution of the Acasta sources as a function of time is depicted in Figure 5. The early-enriched Hadean source of Acasta differentiated at 4350 Ma (see section 5.3 for the model age estimate) from the BSE, which at that time had ε^{143}Nd of -25.3 and ^{142}Nd/^{144}Nd of -27 ppm. The Acasta source evolved with lower ^{143}Nd/^{144}Nd and ^{142}Nd/^{144}Nd than the BSE owing to its low ^{147}Sm/^{144}Nd of 0.1505. Eoarchean Acasta rocks formed at 3960 Ma (based on zircon U-Pb ages) from the enriched Hadean source that had ε^{143}Nd of -18.7 and ^{142}Nd/^{144}Nd of -10 ppm and evolved with ^{147}Sm/^{144}Nd ratios ranging from 0.0900 to 0.1800 (Figure 3). This range in ^{147}Sm/^{144}Nd corresponds to measured values in the Acasta sample suite. The low ^{142}Nd/^{144}Nd of -10 ± 5 ppm inherited by the mafic Acasta rocks did not evolve further because ^{146}Sm was extinct well before the emplacement age of the AGC at 3920–3960 Ma. Acasta rocks were partially reset due to a metamorphic event at 3371 Ma (age of the ^{147}Sm-^{143}Nd errorchron, see Figure 1) in a closed system. Their Nd isotope compositions were homogenized to a mean value of ε^{143}Nd of -7.7 ± 4.6 and ^{142}Nd/^{144}Nd of -10 ± 5 ppm. Acasta rocks eventually evolved with the same ^{147}Sm/^{144}Nd range until today. Sample AG09008 with a ^{142}Nd deficit of -7.4 ppm possibly formed from the same source as the 3960 Ma Acasta rocks, and in such a case the estimated zircon U-Pb age of ca. 3750 Ma would be the age of a metamorphic event to have affected these rocks [*Mojzsis et al.*, 2014].

Overall, this model illustrates the persistence of an early-enriched Hadean reservoir until ~600 Myr after it formed. The felsic Acasta rocks with no resolvable ^{142}Nd deficits likely formed at 3600 Ma (based on zircon U-Pb ages and recent Lu-Hf isotope work) from the Archean BSE and evolved with a low ^{147}Sm/^{144}Nd of ~0.0750. They were intermixed with the older protoliths and also partially reset at 3371 Ma in a closed system, while their U-Pb zircon ages and ^{142}Nd compositions were preserved.

6. Implications

Combined congruous ^{147,146}Sm-^{143,142}Nd and ^{176}Lu-^{176}Hf systematics [*Guitreau et al.*, 2014] for Acasta rocks show that the late Hadean (ca. 3920–3960 Ma) protoliths were derived from a ca. 4350 Ma enriched early Hadean component characterized by unradiogenic Nd and Hf isotope compositions. This component had relatively low Sm/Nd and Lu/Hf ratios and likely does not represent the ultramafic mantle but rather corresponds to a mafic/ultramafic melt stored in the crust [e.g., komatiites; *Blichert-Toft and Arndt*, 1999]. This

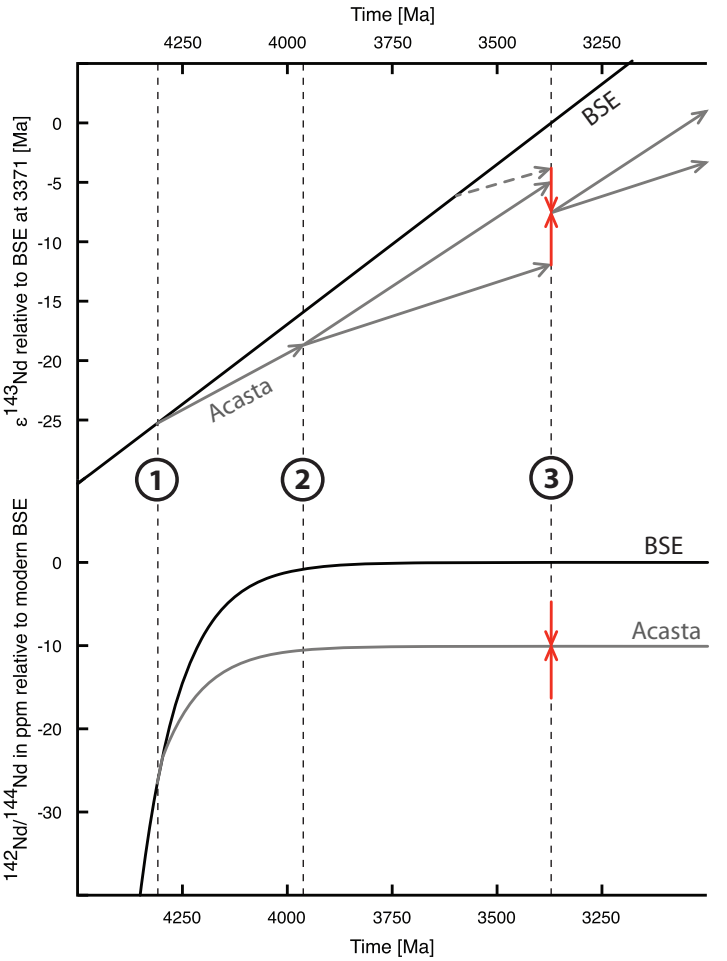

Figure 5. (top) ^{143}Nd/^{144}Nd and (bottom) ^{142}Nd/^{144}Nd evolution diagrams illustrating the Nd isotope evolution of Acasta. BSE and Acasta evolutions are shown in black and gray, respectively. BSE corresponds to the superchondritic composition defined in *Caro and Bourdon* [2010]. (1) Extraction at 4310 Ma of the early-enriched Acasta source from the BSE. (2) Formation at 3960 Ma of Acasta rocks from the early-enriched source. The two arrows represent the samples with the most extreme Sm/Nd ratios. (3) Neodymium isotope equilibration at 3371 Ma of Acasta rocks (red arrows). Felsic Acasta rocks with ^{142}Nd/^{144}Nd identical to BSE formed at 3600 Ma (based on zircon U-Pb ages) from the BSE and evolved with a low ^{147}Sm/^{144}Nd of 0.0750 (dashed arrow).

Hadean crustal source would have had a surface residence time of at least 350 Myr but was ultimately recycled. It is not being sampled today unless it is currently stored in the deeper crust. Younger Paleoarchean (3600 Ma) protoliths for some Acasta rocks are derived from an Archean BSE source that was still able to interact with the Hadean source. *Guitreau et al.* [2014] concluded that the initial Hf isotope compositions of the oldest ca. 3920–3960 Ma Acasta gneisses are representative of their source, which models show can be a ca. 4350 Ma Hadean mafic/ultramafic "primordial" crust instead of the mantle. Zircon xenocrysts with ages of up to ca. 4200 Ma [*Iizuka et al.*, 2006] also crystallized from an early-enriched source that formed in the Hadean [see *Mojzsis et al.*, 2014 for a model of this source], but is likely more evolved than that which carries ^{142}Nd anomalies. Assimilation of such crust, however, does not seem to have significantly influenced the Nd and Hf isotope systematics [cf. *Guitreau et al.*, 2014].

Reworking of old Hadean crust to form new Archean crust is not restricted to Acasta. Early-enriched Hadean reservoirs were also reported by *O'Neil et al.* [2008] and later confirmed by *Roth et al.* [2013] for the ca. 3750 Ma Nuvvuagittuq Supracrustal Belt in Québec (Canada) and even for younger ca. 3400 Ma rocks from Isua in southern West Greenland [*Rizo et al.*, 2012]. In contrast to Acasta, the Nuvvuagittuq [*Roth et al.*, 2013] and Isua [*Rizo et al.*, 2012] terranes yield significantly older model ages of ~4500 Ma. Nuvvuagittuq [*Guitreau et al.*, 2013] and Isua [e.g., *Caro et al.*, 2005] further both have decoupled (incongruous) Nd-Hf isotope systematics that were argued to reflect differentiation of a primordial deep magma ocean. Despite extensive

searches, rocks at Nuvvuagittuq [*Cates and Mojzsis*, 2009; *Cates et al*., 2013] and the Itsaq Gneiss Complex in West Greenland [e.g., *Compston et al*., 1986; *Nutman et al*., 2009] do not preserve pre-3920 Ma zircons [cf. *Mojzsis and Harrison*, 2002]. The early-enriched source found in Acasta is different in several fundamental ways from those reported so far from elsewhere in Earth's oldest cratonic domains. We propose that Acasta may represent a more evolved generation of Hadean crust that emerged after the magma ocean had finished crystallizing and hence did not preserve primitive geochemical evidence for deep magma ocean differentiation.

6.1. The ^{142}Nd Record Through Time: Implications for the Long-Term Evolution of the Mantle-Crust System

The Nd isotope signature of Acasta gneisses represents a useful complement to better understand the Nd isotope evolution of the global mantle-crust system. The presence of ^{142}Nd anomalies in Nuvvuagittuq [*O'Neil et al*., 2008, 2012; *Roth et al*., 2013] and Isua [*Caro et al*., 2006; *Rizo et al*., 2013] together with those now reported here for Acasta suggests that the existence of enriched reservoirs during the Hadean was rather common. The fact that the age of Sm/Nd fractionation predates the age of the rocks shows that these enriched reservoirs were stored for several hundred million years and tapped during subsequent magmatic events. This view is also consistent with the Hf isotopic record preserved in the pre-4000 Ma Jack Hills zircons [*Harrison et al*., 2005; *Blichert-Toft and Albarède*, 2008] that indicates an early age of Lu/Hf fractionation predating the formation of most zircons.

We now examine in greater detail the implications of these observations for the long-term evolution of the mantle-crust system. Using a two-box model for the mantle-crust system, *Caro et al*. [2006] showed that the positive ^{142}Nd anomalies in Archean rocks could be explained by the formation of an early crust with a residence time of about 500 Ma, but no such reservoir with a negative ^{142}Nd anomaly had been identified at the time. One could reasonably question the global significance of the ^{142}Nd observations for the mantle-crust system, however, given that at the time ^{142}Nd anomalies had been found at only one locality (Isua, West Greenland). The discovery of ^{142}Nd anomalies in Acasta from this work, as well as in northern Québec at Nuvvuagittuq [*O'Neil et al*., 2008; *Roth et al*., 2013] and the most ancient components of the Yilgarn craton in Western Australia [*Bennett et al*., 2007] demonstrates that ^{142}Nd anomalies are not restricted to a single locality but likely were widespread in the early Earth. This perspective offers the opportunity to investigate the early mantle-crust differentiation with more detailed modeling and a more extensive data set.

The model used here is a generalization of the box model of *Caro et al*. [2006], allowing the calculation of the statistical distribution of heterogeneities. The Caro model is a two-reservoir model, one reservoir being the crust, the other the depleted mantle. Material is exchanged between these two reservoirs in such a way that the size of the two reservoirs remained unchanged with time. Material is transferred from the crust to the mantle with no change in composition (simple recycling), but material transferred from the mantle to the crust undergoes fractionation, producing a crust enriched in incompatible elements and leaving the mantle depleted. For a given chemical species, the number of moles in each reservoir is described by the following ordinary differential equations:

$$\frac{dx_c}{dt} = -\frac{x_c}{R_c} + \frac{x_m}{R_m} \tag{1}$$

$$\frac{dx_m}{dt} = \frac{x_c}{R_c} - \frac{x_m}{R_m} \tag{2}$$

where x_c and x_m are the number of moles of the species in the crust and mantle reservoirs, respectively. R_c is the residence time in the crustal reservoir, which is the same for every element, and R_m is the residence time of the given species in the mantle reservoir, which is related to the crustal residence time by:

$$R_m = \frac{1-F}{\beta F} R_c \tag{3}$$

where F is the mass of the crustal reservoir relative to that of the total system, and β controls the fractionation of the given species by the melting process, given by:

$$\beta = \frac{1}{F + D(1-F)} \tag{4}$$

where D is the partition coefficient of the element in question. The mean evolution of the system can be found by integrating (1) and (2), and it is straightforward to add terms to include radioactivity. For starting conditions we begin from an initially undifferentiated composition where $x_c(0) = F \cdot x_0$, $x_m(0) = (1\text{-}F) \cdot x_0$ (this differs from *Caro et al*. [2006] who have an initial differentiation event).

The isotope heterogeneity of the mantle reservoir is modeled following the approach of *Rudge et al*. [2005] and *Rudge* [2006] where probability density functions for composition are calculated. The mantle reservoir contains four principal types of heterogeneity: (1) Primitive mantle material that has never left the mantle box (notation: $\langle 1 \rangle$ in what follows); (2) primitive crustal material that was initially in the crust box, moved to the mantle, and then never left the mantle; (3) residue of melting, that was produced as a result of the fractionation process at some time τ in the past and returned to the mantle box; (4) former melt, that was produced as melt during the fractionation event at a time τ in the past, went to the crust, and now has been returned to the mantle. It is assumed that the fractionation process completely homogenizes, producing crustal material with uniform composition and thus no memory is retained of events before the most recent melting event.

The first step in the statistical model is to determine the relative amounts of each of these four types of heterogeneity, and for types 3 and 4 their distribution of ages. To determine the distribution of ages, it is natural to think of running the model backward in time from the present day. Any nonprimitive mantle material was either (1) recycled from the crust or (2) a residue of melting. If we treat all transfer processes as Poisson processes, then the distribution of waiting times are given by exponential distributions,

$$\hat{T}_1 \sim \mathrm{Exp}(1/\mu_1) \tag{5}$$

$$\hat{T}_2 \sim \mathrm{Exp}(1/\mu_2) \tag{6}$$

where $\hat{T}_1$ and $\hat{T}_2$ are random variables corresponding to the two transfer processes described above. The means μ_1 and μ_2 of these exponential distributions are given by:

$$\mu_1 = \frac{1-F}{F} R_c \tag{7}$$

$$\mu_2 = R_c \tag{8}$$

Of the material that came from the crust, the waiting time distribution in the crust follows another exponential distribution:

$$\hat{T}_3 \sim \mathrm{Exp}(1/\mu_3) \tag{9}$$

$$\mu_3 = R_c \tag{10}$$

The age distribution of mantle material (the time since the last melting event) is given by:

$$\hat{T} = \min\left(\hat{T}_1 + \hat{T}_3, \hat{T}_2, \tau_s\right) \tag{11}$$

where the $\hat{T}_1 + \hat{T}_3$ term represents material that was made as melt to form crust and then subsequently recycled; the $\hat{T}_2$ term represents material formed as residue. Primitive material is assigned an age of τ_s, the time elapsed since the beginning of the model. The proportion of each of the four types of heterogeneity and their ages can be expressed in terms of the following probabilities,

$$P(\langle 1 \rangle) = P\left(\hat{T}_1 > \tau_s \cap \hat{T}_2 > \tau_s\right), \tag{12}$$

$$P(\langle 2 \rangle) = P\left(\hat{T}_1 < \hat{T}_2 \cap \hat{T}_1 > \tau_s \cap \hat{T}_1 + \hat{T}_3 > \tau_s\right) \tag{13}$$

$$P(\langle 3\rangle \cap \hat{T}=t)=P(\hat{T}_1 > \hat{T}_2 \cap \hat{T}_2=t), \tag{14}$$

$$P(\langle 4\rangle \cap \hat{T}=t)=P(\hat{T}_1 < \hat{T}_2 \cap \hat{T}_1 < \tau_s \cap \hat{T}_1+\hat{T}_3=t), \tag{15}$$

where the final two probabilities are probability densities for a given age. Note that these probabilities must sum to 1, namely,

$$P(\langle 1\rangle)+P(\langle 2\rangle)+\int_0^{\tau_s} P(\langle 3\rangle \cap \hat{T}=t)dt+\int_0^{\tau_s} P(\langle 4\rangle \cap \hat{T}=t)dt=1 \tag{16}$$

The probabilities can be calculated explicitly as:

$$P(\langle 1\rangle)=e^{-\tau_s/\bar{\mu}}, \tag{17}$$

$$P(\langle 2\rangle)=\frac{\bar{\mu}}{\mu_1}\frac{\mu_3}{\bar{\mu}-\mu_3}\left(e^{-\tau_s/\bar{\mu}}-e^{-\tau_s/\mu_3}\right), \tag{18}$$

$$P(\langle 3\rangle \cap \hat{T}=t)=\frac{1}{\mu_2}e^{-t/\bar{\mu}} \tag{19}$$

$$P(\langle 4\rangle \cap \hat{T}=t)=\frac{\bar{\mu}}{\mu_1}\frac{1}{\bar{\mu}-\mu_3}\left(e^{-t/\bar{\mu}}-e^{-t/\mu_3}\right) \tag{20}$$

where:

$$\frac{1}{\bar{\mu}}=\frac{1}{\mu_1}+\frac{1}{\mu_2} \tag{21}$$

It is straightforward to calculate the composition of melt or residue produced at any time in the model by integration of (1) and (2). Combining this with the probabilities above allows one to calculate arbitrary moments of the chemical composition of the mantle reservoir, including the variance.

When sampling from the mantle, we do not see the full range of heterogeneity because it is altered through melting and mixing. We model this in a very simple way using the "N parameter" of *Rudge et al.* [2005, 2013]. For N = 1 there is no mixing; for large N there is intense mixing. N characterizes the reduction in variance: mixing reduces the variance in concentrations by a factor of 1/N. The effect of mixing on ratio quantities is more subtle (see discussion in *Rudge et al.* [2005]). When calculating the variance for isotopic ratios, the asymptotic expression given in (B.6) of *Rudge* [2006] has been used, which predicts that for large N the variance in isotopic ratios should also scale with 1/N. The N parameterization is a fairly crude model of mixing, and a more sophisticated model would take account of the fact that the amount of mixing will evolve with time [e.g., *Kellogg et al.*, 2002].

By adding the new observations that were not available to *Caro et al.* [2006], it is now possible to get tighter and rigorous constraints on the rate of crustal growth and recycling. It turns out that the crustal residence time R_c is the most important parameter determining the disappearance of positive anomalies in the mantle. By having preservation of crust carrying negative ^{142}Nd anomalies as is the case in Acasta, the complementary depleted mantle with positive anomalies accordingly can survive over longer periods of time. As shown in Figures 6 and 7, the observations can be matched with a crustal residence time of approximately 750 Ma, which is in good agreement with the determination of *Caro et al.* [2006]. This determination is based both on the ^{142}Nd and ^{143}Nd record, unlike that of *Caro et al.* [2006]. The model illustrated in Figure 7 (bottom) also shows that mantle heterogeneity as characterized by the standard deviation of ^{142,143}Nd for a given value of the mixing parameter N is largely controlled by the crustal residence time and that the existence of heterogeneity is not only a function of the mixing parameter N. In this context, based on the preservation of positive or negative ^{142}Nd anomalies in the mantle as shown in Figure 7, it is difficult to infer a particular value of the mixing time scale. For example, as argued in *Rizo et al.* [2012], the possible existence

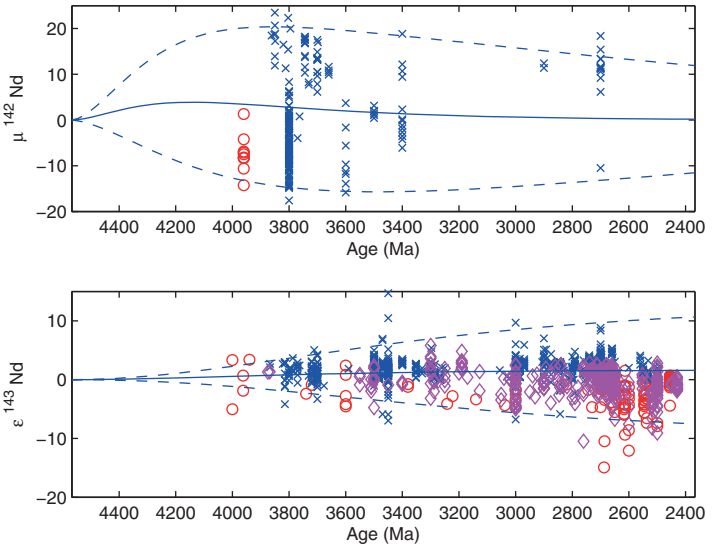

Figure 6. Evolution of Nd isotopic heterogeneity through time in the mantle. (top) $^{142}Nd/^{144}Nd$ (shown as $\mu^{142}Nd$) and (bottom) $^{143}Nd/^{144}Nd$ (shown as $\varepsilon^{143}Nd$). Solid blue lines show the mean evolution of the model mantle, dashed blue lines show $\pm 2\sigma$ deviation. Symbols show observations with crustal-derived reservoirs as red circles; mantle reservoirs as blue crosses; and mixed reservoirs as purple diamonds. The crustal-derived reservoirs represent a source of heterogeneity in the mantle. The observations are broadly consistent with a crustal residence time of around 750 Myr as used here. The mixing parameter is N = 25. All parameter values used in this calculation can be found as supporting information in Table S2. Data sources are given as supporting information in Tables S3 and S4.

of negative ^{142}Nd anomalies reported in ca. 3400 Ma Isua rocks, does not necessarily imply a 1 Gyr mixing time scale.

The recent discovery by *Debaille et al*. [2013] of a positive ^{142}Nd anomaly in 2660 Ma komatiites from the Abitibi Greenstone Belt represents an interesting challenge to numerical models of mantle heterogeneity since it has been argued in the past that rapid stirring in the early Earth had erased initial heterogeneities

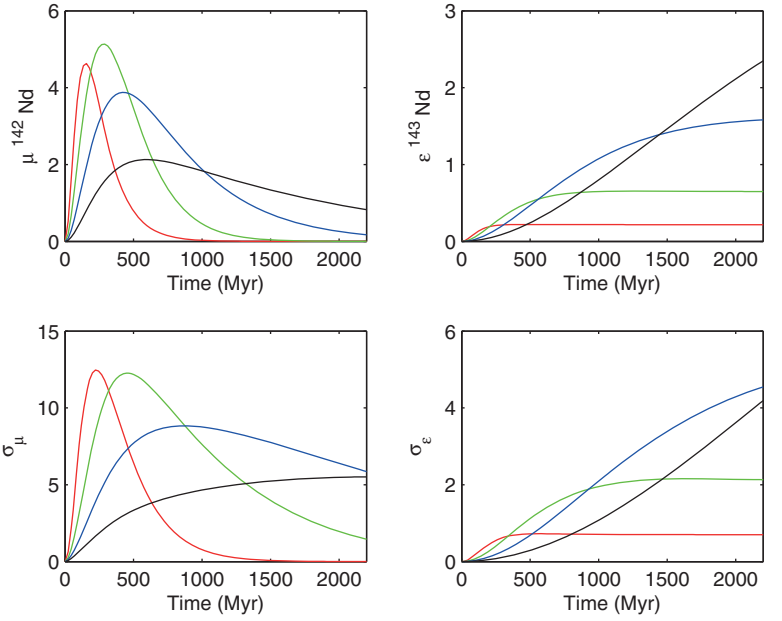

Figure 7. Model evolution through time for different values of the crustal residence time R_c. Red curve $R_c = 100$ Myr, green curve $R_c = 300$ Myr, blue curve $R_c = 750$ Myr, and black curve $R_c = 2000$ Myr. (top) The mean evolution of $^{142}Nd/^{144}Nd$ and $^{143}Nd/^{144}Nd$ and (bottom) the standard deviation evolution.

[e.g., *Blichert-Toft and Albarède*, 1994; *Caro et al*., 2006]. *Debaille et al*. [2013] used this to argue for a stagnant-lid convective regime during the Archean, which would have helped preserve mantle heterogeneities over longer time scales than mobile-lid tectonics. They argued based on a model of heterogeneities in the convective mantle that mobile-lid tectonics rapidly destroy early formed heterogeneites in the mantle. This means that their "late" ^{142}Nd anomaly at 2660 Ma should have disappeared earlier. However, they did not consider the dynamics of crustal reservoirs in their model, as in this study.

The presence of positive ^{142}Nd anomalies in mantle-derived rocks long after all ^{146}Sm has decayed away indicates that either the mantle was heterogeneous and inefficiently mixed or an early crustal reservoir was preserved until that time, which means, from mass balance arguments, that the mantle had to stay depleted accordingly (with high Sm/Nd). Our modeling illustrated in Figures 6 and 7 shows that as long as the residence time of the crust remains long enough (according to Figure 6, about 750 Myr), positive ^{142}Nd anomalies in the mantle can be preserved over long time scales. In this case, what controls the existence of an anomaly is the storage in the crust of a reservoir with a negative anomaly, which is conceptually different from preserving heterogeneity in the mantle due to incomplete stirring. Thus, the observations of *Debaille et al*. [2013] do not require that mantle convection operated with a stagnant lid. The positive ^{142}Nd anomaly found at 2660 Ma does not necessarily imply "mantle heterogeneity" at this time (although this cannot be ruled out per se) and more observations of rocks of similar age at different localities would be needed to support such a hypothesis.

In summary, our modeling of the ^{142}Nd evolution of the mantle-crust system shows that the preservation (and recycling) of Hadean crust for ~750 Myr after its formation can adequately explain the observations made on actual rocks and there is no a priori requirement to call for a different mode of mantle convection.

6.2. Vestiges of Magma Ocean Crystallization

The remarkably old age of Sm/Nd fractionation inferred for Isua [*Caro et al*., 2003; *Boyet et al*., 2003] has been a major argument in favor of the possibility that it may record magma ocean crystallization. It was pointed out by *Caro et al*. [2005] that the unusual pattern of Sm/Nd and Lu/Hf fractionation observed in Isua indicated the presence of a mixture of Mg-perovskite and Ca-perovskite, an interpretation reemphasized by *Rizo et al*. [2011]. In the following, we examine both the Acasta and Isua records from the perspective of putative magma ocean crystallization in the earliest Hadean.

The process of magma ocean crystallization according to the early work of *Solomatov and Stevenson* [1993a, 1993b], later reviewed by *Solomatov* [2007], is complex and comprehensive modeling of the process and its consequences for Sm/Nd and Lu/Hf fractionation is not possible. To mention just some of these complexities, *Mosenfelder et al*. [2007], followed by *Fiquet et al*. [2010], argued for middepth crystallization of a terrestrial magma ocean, although earlier studies considered bottom to mid-depth crystallization. In addition, except for plagioclase, which is a minor phase in the Earth's mantle, most minerals were considered to be denser than the melt. However, the relative density of melt and minerals has recently been a topic of debate [*Andrault et al*., 2010; *Thomas et al*., 2012; *Nomura et al*., 2011] and their relative buoyancies have been shown to be a function of pressure and melt composition. In such a context, it is difficult to construct a realistic model for magma ocean crystallization with the aim of predicting trace element fractionation, such as the differentiation of the key Sm/Nd and Lu/Hf ratios. For the sake of simplicity, we determined the melt and solid compositions corresponding to each mineral assemblage crystallizing in the lower and upper parts of the mantle (with the exclusion of the postperovskite domain) and calculated the Lu/Hf and Sm/Nd ratios of melts and solids for various degrees of equilibrium crystallization using the partition coefficients determined by *Corgne and Wood* [2005], *Corgne et al*. [2005], and *Liebske et al*. [2005] or *Hauri et al*. [1994] for the upper mantle. The results are plotted in Figure 8 and illustrate clearly that for Isua crystallization of a mixture of Mg-perovskite and Ca-perovskite is required, while the Nd and Hf isotope observations for Acasta can be explained by melting of a depleted upper mantle mineral assemblage (70% olivine, 25% orthopyroxene, and 5% clinopyroxene). This outcome further emphasizes the peculiarity of the Isua Nd and Hf isotope observations compared to those of Acasta. The model age of Sm/Nd and Lu/Hf fractionation for Acasta is 4350 Ma, which is younger than that for Isua (4450–4500 Ma) and hence could account for the isotopic differences between these two localities. One can also compare the cases of Acasta and Isua to the observations in Nuvvuagittuq. The model age of Sm/Nd and Lu/Hf fractionation for Nuvvuagittuq is 4480 Ma, but following an early fractionation event similar to that in Isua, the source of Nuvvuagittuq was later

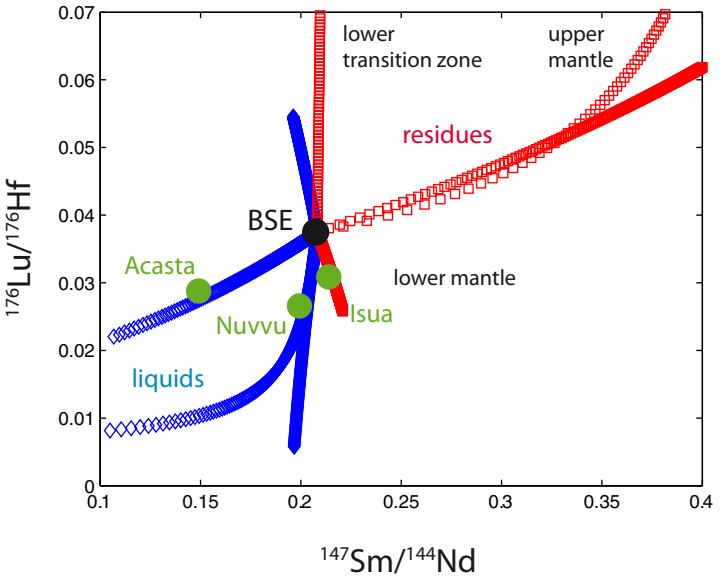

Figure 8. $^{176}Lu/^{177}Hf$ versus $^{147}Sm/^{144}Nd$ illustrating the effect of magma ocean crystallization starting from a bulk silicate Earth composition with superchondritic Sm/Nd and Lu/Hf ratios as in *Caro and Bourdon* [2010]. The composition of residual melts is shown with blue diamonds, while crystallized solids are shown as red squares. The model assumes equilibrium crystallization and the partition coefficients were taken from *Corgne et al.* [2005] and *Liebske et al.* [2005] and compiled by *Caro et al.* [2005]. Four mineral assemblages for the crystallization of lower mantle and lower and upper transition zone as in *Caro et al.* [2005] were considered. The best fit for the Acasta data is obtained for an upper mantle with 70% olivine, 25% orthopyroxene, and 5% clinopyroxene. $^{176}Lu/^{177}Hf$ versus $^{147}Sm/^{144}Nd$ for Acasta, Nuvvuagittuq (Nuvvu), and Isua source material were calculated using initial $^{176}Hf/^{177}Hf$ versus $^{142}Nd/^{144}Nd$ as explained in section 5.3. The Nd and Hf isotope observations for Isua can be accounted for by crystallization of a lower mantle assemblage, while those for Acasta correspond to upper mantle melting of a depleted source.

refertilized, which obscured the initial pattern of Sm/Nd and Lu/Hf fractionation (see Figure 8), as explained in *Guitreau et al.* [2013]. Altogether, this indicates that by about 4350 Ma, the terrestrial magma ocean had solidified (Isua & Nuvvuagittuq) and "normal" crust production by upper mantle melting began to take place (Acasta). This 4350 Ma age matches that of the oldest Hadean detrital zircons recovered from metasedimentary belts in the Yilgarn craton [e.g., *Mojzsis et al.*, 2001; *Wilde et al.*, 2001; *Valley et al.*, 2014] for which Hf isotope signatures are similar to that of CHUR, and hence BSE. These two reservoirs had essentially identical Hf isotope compositions at 4350 Ma. We suggest that this recurring Hadean age may represent the initiation of Earth's resurfacing processes.

7. Conclusions

This study presents the first analysis of the Acasta gneiss complex to report significant negative ^{142}Nd anomalies consistent with the formation of an early crustal reservoir during Hadean times. Notably, Acasta rocks with the greatest deficits in ^{142}Nd are also the most mafic. Early crust enrichment documented by ^{142}Nd deficits of up to 15 ppm in Hadean-Eorchean rocks from Acasta (this study), Nuvvuagittuq [*O'Neil et al.*, 2008; *Roth et al.*, 2013], and Isua [*Rizo et al.*, 2012] is complementary to early mantle depletion documented by ^{142}Nd excesses of up to 15 ppm in Archean rocks from elsewhere in the Itsaq Gneiss Complex of West Greenland [*Boyet et al.*, 2003; *Caro et al.*, 2003, 2006; *Rizo et al.*, 2011] and the Narryer Gneiss Complex in Western Australia [*Bennett et al.*, 2007]. The model age of extraction for the precursor of the oldest Acasta gneisses, which corresponds to the time of Sm/Nd fractionation, is approximately 4300 Ma. This model age is younger than that inferred for Isua and Nuvvuagittuq rocks (approximately 4500 Ma). Accordingly, the patterns of Sm/Nd and Lu/Hf fractionation are distinct in these localities. Isua is consistent with the fractionation of lower mantle phases, indicating a deep magma ocean environment, whereas Acasta reflects melt extraction from the upper mantle.

Examination of the ^{142}Nd record through time for the terrestrial mantle-crust system shows that it can be explained by early crust extraction during the first few hundred Myr of Earth history followed by "slow"

recycling of this early crust into the mantle with a crustal residence time estimated to be 750 Myr. These observations do not require a slow stirring time for the mantle, nor do they require a modification of its convective mode. More data forthcoming from other ancient terranes are needed to fully resolve this issue.

Acknowledgments

We are indebted to W. Bleeker (Geological Survey of Canada) for discussions of the geological context of the Acasta rocks and advice in the course of field studies. N.L. Cates (University of Colorado) provided valuable data to unravel the geochemical relations of the samples. Insightful discussions with S. Labrosse, S. Jacobsen, and Y. Ueno helped to forge the ideas presented herein. This project was funded by an ETH internal grant to B.B. We thank C. Maden for maintenance of the mass spectrometer. S.J.M. acknowledges support from the NASA Exobiology and Evolutionary Biology Program (Investigating the Hadean Earth) and the NASA Lunar Science Institute (Center for Lunar Origin and Evolution, CLOE). Additional support to S.J.M. came from the Laboratoire de Géologie de Lyon, Université Claude Bernard Lyon 1, and a Distinguished Professorship awarded by the Hungarian Academy of Sciences. J.B.T. received support from the French Agence Nationale de la Recherche (grant ANR-10-BLAN-0603 M&Ms—Mantle Melting—Measurements, Models, Mechanisms). We are especially grateful for the invaluable logistical assistance for work in the Acasta Gneiss Complex provided by the Geological Survey of Canada and the Northwest Territories Geoscience Field Office in Yellowknife by J. Ketchum and D. Irwin. We also thank an anonymous reviewer for providing a constructive review.

References

Andrault, D., S. Petitgirard, G. Lo Nigro, J. L. Devidal, G. Veronesi, G. Garbarino, and M. Mezouar (2010), Solid-liquid iron partitioning in Earth's deep mantle, *Nature*, *487*, 354–357.

Bennett, V. C., A. P. Nutman, and M. T. McCulloch (1993), Nd isotopic evidence for transient, highly depleted mantle reservoirs in the early history of the Earth, *Earth Planet. Sci. Lett.*, *119*, 299–317.

Bennett, V. C., A. D. Brandon, and A. P. Nutman (2007), Coupled ^{142}Nd-^{143}Nd isotopic evidence for Hadean mantle dynamics, *Science*, *318*, 1907–1910.

Bleeker, W., and R. Stern (1997), The Acasta gneisses: An imperfect sample of Earth's oldest crust, in *Slave-Northern Cordillera Lithospheric Evolution (SNORCLE) Transect and Cordilleran Tectonics Workshop Meeting*, edited by F. Cook and P. Erdmer, pp. 32–35, *Lithosphere Rep.* 56.

Blichert-Toft, J., and F. Albarède (1994), Short-lived chemical heterogeneities in the Archean mantle with implications for mantle convection, *Science*, *263*, 1593–1596.

Blichert-Toft, J., and F. Albarède (2008), Hafnium isotopes in Jack Hills zircons and the formation of the Hadean crust, *Earth Planet. Sci. Lett.*, *265*, 686–702.

Blichert-Toft, J., and N. T. Arndt (1999), Hf isotope compositions of komatiites, *Earth Planet. Sci. Lett.*, *171*, 439–451.

Bouvier, A., J. D. Vervoort, and P. J. Patchett (2008), The Lu-Hf and Sm-Nd isotopic composition of CHUR: Constraints from unequilibrated chondrites and implications for the bulk composition of terrestrial planets, *Earth Planet. Sci. Lett.*, *273*, 48–57.

Bowring, S. A., and T. B. Housh (1995), The Earth's early evolution, *Science*, *269*, 1535–1540.

Bowring, S. A., and I. S. Williams (1999), Priscoan (4.00–4.03 Ga) orthogneisses from NW Canada, *Contrib. Mineral. Petrol.*, *134*, 3–16.

Bowring, S. A., I. S. Williams, and W. Compston (1989a), 3.96 Ga gneisses from the Slave Province, NWT, Canada, *Geology*, *17*, 971–975.

Bowring, S. A., J. E. King, T. B. Housh, C. E. Isachsen, and F. A. Podsek (1989b), Neodymium and lead isotope evidence for enriched early Archean crust in North America, *Nature*, *340*, 222–225.

Bowring, S. A., T. B. Housh, and C. E. Isachsen (1990), The Acasta Gneisses: Remnant of Earth's early crust, in *Origin of the Earth*, edited by H. E. Newsom and J. H. Jones, pp. 319–343, Oxford Univ. Press, Oxford, U. K.

Boyet, M., J. Blichert-Toft, M. Rosing, M. Storey, P. Télouk, and F. Albarède (2003), Nd-142 evidence for early Earth differentiation, *Earth Planet. Sci. Lett.*, *214*, 427–442.

Caro, G., and B. Bourdon (2010), Non-chondritic Sm/Nd ratio in the terrestrial planets: Consequences for the geochemical evolution of the mantle crust system, *Geochim. Cosmochim. Acta*, *74*, 3333–3349.

Caro, G., B. Bourdon, J. L. Birck, and S. Moorbath (2003), ^{146}Sm-^{142}Nd evidence from Isua metamorphosed sediments for early differentiation of the Earth's mantle, *Nature*, *423*, 428–432.

Caro, G., B. Bourdon, B. J. Wood, and S. Corgne (2005), Trace element fractionation in Hadean mantle generated by melt segregation from a magma ocean, *Nature*, *436*, 246–249.

Caro, G., B. Bourdon, J. L. Birck, and S. Moorbath (2006), High-precision ^{142}Nd/^{144}Nd measurements in terrestrial rocks: Constraints on the early differentiation of the Earth's mantle, *Geochim. Cosmochim. Acta*, *70*, 164–191.

Cates, N. L., and S. J. Mojzsis (2009), Metamorphic zircon, trace elements and Neoarchean metamorphism in the ca. 3.75 Ga Nuvvuagittuq supracrustal belt, Québec (Canada), *Chem. Geol.*, *261*, 99–114.

Cates, N. L., K. Ziegler, A. K. Schmitt, and S. J. Mojzsis (2013), Reduced, reused and recycled: Detrital zircons define a maximum age for the Eoarchean (ca. 3750–3780 Ma) Nuvvuagittuq Supracrustal Belt, Québec (Canada), *Earth Planet. Sci. Lett.*, *362*, 283–293.

Compston, W., P. D. Kinny, I. S. Williams, and J. J. Foster (1986), The age and Pb loss behaviour of zircons from the Isua supracrustal belt as determined by ion microprobe, *Earth Planet. Sci. Lett.*, *80*, 71–81.

Corgne, A., and B. J. Wood (2005), Trace element partitioning and substitution mechanisms in calcium perovskites, *Contrib. Mineral. Petrol.*, *149*, 85–97.

Corgne, A., C. Liebske, B. J. Wood, D. C. Rubie, and D. J. Frost (2005), Silicate perovskite-melt partitioning of trace elements and geochemical signature of a deep perovskitic reservoir, *Geochim. Cosmochim. Acta*, *69*, 485–496.

Debaille, V., C. O'Neill, A. D. Brandon, P. Haenecour, Q.-Z. Yin, N. Mattielli, and A. H. Treiman (2013), Stagnant-lid tectonics in early Earth revealed by ^{142}Nd variations in late Archean rocks, *Earth Planet. Sci. Lett.*, *373*, 83–92.

Fiquet, G., A. L. Auzende, J. Siebert, A. Corgne, H. Bureau, and G. Garbarino (2010), Melting of peridotite to 140 gigapascals, *Science*, *329*, 1516–1518.

Guitreau, M., J. Blichert-Toft, H. Martin, S. J. Mojzsis, and F. Albarède (2012), Hafnium isotope evidence from Archean granitic rocks for deep-mantle origin of continental crust, *Earth Planet. Sci. Lett.*, *337*, 211–223.

Guitreau, M., J. Blichert-Toft, S. J. Mojzsis, A. S. G. Roth, and B. Bourdon (2013), A legacy of Hadean silicate differentiation inferred from Hf isotopes in Eoarchean rocks of the Nuvvuagittuq supracrustal belt (Québec, Canada), *Earth Planet. Sci. Lett.*, *362*, 171–181.

Guitreau, M., J. Blichert-Toft, S. J. Mojzsis, A. S. G. Roth, B. Bourdon, N. L. Cates, and W. Bleeker (2014), Lu-Hf isotope systematics of the Hadean-Eoarchean Acasta Gneiss Complex (Northwest Territories, Canada), *Geochim. Cosmochim. Acta*, *135*, 251–269.

Harrison, T. M., J. Blichert-Toft, W. Müller, F. Albarède, P. Holden, and S. J. Mojzsis (2005), Heterogeneous Hadean hafnium: Evidence of continental crust at 4.4 to 4.5 Ga, *Science*, *310*, 1947–1950.

Hauri, E. H., T. P. Wagner, and T. L. Grove (1994), Experimental and natural partitioning of Th, U, Pb and other trace elements between garnet, clinopyroxene and basaltic melts, *Chem. Geol.*, *117*, 149–166.

Iizuka, T., K. Horie, T. Komiya, S. Maruyama, T. Hirata, H. Hidaka, and B. F. Windley (2006), 4.2 Ga zircon xenocryst in an Acasta gneiss from northwestern Canada: Evidence for early continental crust, *Geology*, *34*, 245–248.

Iizuka, T., T. Komiya, and S. Maruyama (2007), The early Archean Acasta Gneiss Complex: Geological, geochronological and isotopic studies and implications for early crustal evolution, in *Developments in Precambrian Geology*, vol. 15, edited by M. J. van Kranendonk, R. H. Smithies, and V. C. Bennett, chap. 3.1., pp. 127–147, Elsevier B.V.

Iizuka, T., T. Komiya, S. P. Johnson, Y. Kon, S. Maruyama, and T. Hirata (2009), Reworking of Hadean crust in the Acasta gneisses, northwestern Canada: Evidence from in-situ Lu-Hf isotope analysis of zircon, *Chem. Geol.*, *259*, 230–239.

Kellogg, J. B., S. B. Jacobsen, and R. J. O'Connell (2002), Modelling the distribution of isotopic ratios in geochemical reservoirs, *Earth Planet. Sci. Lett.*, *204*, 183–202.
King, S. E. (1985), Structure of the metamorphic-internal zone, Northern Wopmay Orogen, Northwest Territories, Canada, PhD thesis, Queens University, Kingston, Ontario, Canada, p. 208.
Kinoshita, N., et al. (2012), A shorter ^{146}Sm half-life measured and implications for ^{146}Sm–^{142}Nd chronology in the solar system, *Science*, *335*, 1614–1617.
Liebske, C., A. Corgne, D. J. Frost, D. C. Rubie, and B. J. Wood (2005), Compositional effects on element partitioning between Mg-silicate perovskite and silicate melts, *Contrib. Mineral. Petrol.*, *149*, 113–128.
McCulloch, M. T., and V. C. Bennett (1993), Evolution of the early Earth: Constraints from ^{143}Nd-^{142}Nd isotopic systematics, *Lithos*, *30*, 237–255.
Mojzsis, S. J., and T. M. Harrison (2002), Establishment of a 3.83 Ga magmatic age for the Akilia tonalite (southern West Greenland), *Earth Planet. Sci. Lett.*, *202*, 563–576.
Mojzsis, S. J., T. M. Harrison, and R. T. Pidgeon (2001), Oxygen-isotope evidence from ancient zircons for liquid water at the Earth's surface 4,300 Myr ago, *Nature*, *409*, 178–181.
Mojzsis, S. J., N. L. Cates, G. Caro, D. Trail, O. Abramov, M. Guitreau, J. Blichert-Toft, M. D. Hopkins, and W. Bleeker (2014), Component geochronology in the polyphase ca. 3920 Ma Acasta Gniess, *Geochim. Cosmochim. Acta*, *133*, 68–96.
Moorbath, S., M. J. Whitehouse, and B. S. Kamber (1997), Extreme Nd-isotope heterogeneity in the early Archaean—Fact or fiction? Case histories from northern Canada and West Greenland, *Chem. Geol.*, *135*, 213–231.
Mosenfelder, J. L., P. D. Asimow, and T. J. Ahrens (2007), Thermodynamic properties of Mg_2SiO_4 liquid at ultra-high pressures from shock measurements to 200 GPa on forsterite and wadsleyite, *J. Geophys. Res.*, *112*, B06208, doi:10.1029/2006JB004364.
Nomura, R., H. Ozawa, S. Tateno, K. Hirose, J. Hernlund, S. Muto, H. Ishii, and N. Hiraoka (2011), Spin crossover and iron-rich silicate melt in the Earth's deep mantle, *Nature*, *473*, 199–203.
Nutman, A. P., C. R. L. Friend, and S. Paxton (2009), Detrital zircon sedimentary provenance ages for the Eoarchean Isua Supracrustal Belt southern West Greenland: Juxtaposition of an imbricated ca. 3700 Ma juvenile arc against an older complex with 3920-3760 Ma components, *Precambrian Res.*, *172*, 212–233.
O'Neil, J., R. W. Carlson, D. Francis, and R. K. Stevenson (2008), Neodymium-142 evidence for Hadean mafic crust, *Science*, *321*, 1828–1831.
O'Neil, J., R. W. Carlson, J.-L. Paquette, and D. Francis (2012), Formation age and metamorphic history of the Nuvvuagittuq greenstone belt, *Precambrian Res.*, *220–221*, 23–44.
Rehkämper, M., M. Gärtner, S. J. G. Galer, and S. L. Goldstein (1996), Separation of Ce from other rare-earth elements with application to Sm–Nd and La–Ce chronometry, *Chem. Geol.*, *129*, 201–208.
Rizo, H., M. Boyet, J. Blichert-Toft, and M. Rosing (2011), Combined Nd and Hf isotope evidence for deep-seated source of Isua lavas, *Earth Planet. Sci. Lett.*, *312*, 267–279.
Rizo, H., M. Boyet, J. Blichert-Toft, J. O'Neil, M. Rosing, and J. L. Paquette (2012), The elusive Hadean enriched reservoir revealed by ^{142}Nd deficits in Isua Archaean rocks, *Nature*, *491*, 96–100.
Rizo, H., M. Boyet, J. Blichert-Toft, and M. Rosing (2013), Early mantle dynamics inferred from ^{142}Nd variations in Archean rocks from southwest Greenland, *Earth Planet. Sci. Lett.*, *377–378*, 324–335.
Roth, A. S. G., B. Bourdon, S. J. Mojzsis, M. Touboul, P. Sprung, M. Guitreau, and J. Blichert-Toft (2013), Inherited ^{142}Nd anomalies in Eoarchean protoliths, *Earth Planet. Sci. Lett.*, *361*, 50–57.
Rudge, J. F. (2006), Mantle pseudo-isochrons revisited, *Earth Planet. Sci. Lett.*, *249*, 494–513.
Rudge, J. F., D. McKenzie, and P. H. Haynes (2005), A theoretical approach to understanding the isotopic heterogeneity of mid-ocean ridge basalt, *Geochim. Cosmochim. Acta*, *69*, 3873–3887.
Rudge, J. F., J. Maclennan, and A. Stracke (2013), The geochemical consequences of mixing melts from a heterogeneous mantle, *Geochim. Cosmochim. Acta*, *114*, 112–143.
Sano, Y., K. Terada, H. Hidaka, K. Yokoyama, and A. P. Nutman (1999), Palaeoproterozoic thermal events recorded in the ~4.0 Ga Acasta gneiss, Canada: Evidence from SHRIMP U-Pb dating of apatite and zircon, *Geochim. Cosmochim. Acta*, *63*, 899–905.
Solomatov, V. S. (2007), Magma oceans and primordial mantle differentiation, in *Treatise on Geophysics*, vol. 9, edited by G. Schubert, pp. 91–120, Elsevier, Amsterdam, Netherlands.
Solomatov, V. S., and D. J. Stevenson (1993a), Suspension in convective layers and style of differentiation of a terrestrial magma ocean, *J. Geophys. Res.*, *98*, 5375–5390.
Solomatov, V. S., and D. J. Stevenson (1993b), Nonfractional crystallization of a terrestrial magma ocean, *J. Geophys. Res.*, *98*, 5391–5406.
St-Onge, M. R., J. E. King, and A. E. Lalonde (1988), Geology, east-central Wopmay Orogen, district of Mackenzie, Northwest Territories, *Geol. Surv. of Can., Open-file Rep. 1923*, Natural Resources Canada, sheets 3, scale 1:125,000.
Stern, R. A., and W. Bleeker (1998), Age of the world's oldest rocks refined using Canada's SHRIMP: The Acasta Gneiss Complex, Northwest Territories, *Geosci. Can.*, *25*, 27–31.
Thomas, C. W., Q. Liu, C. B. Agee, P. D. Asimow, and R. A. Lange (2012), Multi-technique equation of state for Fe_2SiO_4 melt and the density of Fe-bearing silicate melts from 0 to 161 GPa, *J. Geophys. Res.*, *117*, B10206, doi:10.1029/2012JB009403.
Valley, J. W., A. J. Cavosie, T. Ushikubo, D. A. Reinhard, D. F. Lawrence, D. J. Larson, T. F. Kelly, S. A. Wilde, D. E. Moser, and M. J. Spicuzza (2014), Hadean age for a post-magma-ocean zircon confirmed by atom-probe tomography, *Nat. Geosci.*, *7*, 219–223.
Whitehouse, M. J., T. F. Nagler, S. Moorbath, J. D. Kramers, B. S. Kamber, and R. Frei (2001), Priscoan (4.00–4.03 Ga) orthogneisses from northwestern Canada – by Samuel A. Bowring and Ian S. Williams: Discussion, *Contrib. Mineral. Petrol.*, *141*, 248–250.
Wilde, S. A., J. W. Valley, W. H. Peck, and C. M. Graham (2001), Evidence from detrital zircons for the existence of continental crust and oceans 4.4 Gyr ago, *Nature*, *409*, 175–178.
Williams, I. S., W. Compston, S. A. Bowring, and T. Housh (1992), The age and history of the Acasta gneisses, Canada: An ion microprobe zircon study, *EOS., Trans. AGU*, *73*, 324.